CHEMISTRY
A EUROPEAN JOURNAL

DOI: 10.1002/chem.200800277

Selectivity of Neutral/Weakly Basic P1 Group Inhibitors of Thrombin and Trypsin by a Molecular Dynamics Study

Emilia L. Wu,[a] KeLi Han,*[a] and John Z. H. Zhang*[b, c]

Abstract: Molecular dynamics (MD) simulations followed by molecular mechanics generalized Born surface area (MM-GBSA) analyses have been carried out to study the selectivity of two neutral and weakly basic P1 group inhibitors (177 and CDA) to thrombin and trypsin. Detailed binding free energies between these inhibitors and individual protein residues are calculated by using a per-residue basis decomposition method. The analysis of the detailed interaction energies provides insight on the protein–inhibitor-binding mechanism and helps to elucidate the basis for achieving selectivity through interpretation of the structural and energetic results from the simulations. The study shows that the dominant factor of selectivity for both inhibitors is van der Waals energy, which suggests better shape complementarity and packing with thrombin. Nonpolar solvation free energy and total entropy contribution are also in favor of selectivity, but the contributions are much smaller. Binding mode and structural analysis show that 177 binds to thrombin and trypsin in a similar binding mode. In contrast, the CDA binds to thrombin and trypsin in very different modes.

Keywords: molecular dynamics · molecular mechanics · selectivity · thrombin · trypsin

Introduction

Owing to its remarkable variety of functions in homeostasis and thrombosis, thrombin has been a special target for molecular drug design. A number of medically important disorders are related to thrombin. Thromboembolic disorders are the major cause of morbidity and mortality in the developed world. Several acute diseases including deep venous thrombosis, pulmonary embolism, unstable angina, restenosis following angioplasty, and arterial thrombosis are also caused by undesired blood-clotting events.[1,2] The clinical syndromes of thromboembolism are triggered by an excessive stimulation of the coagulation cascade.[3–6] Two crucial steps in the cascade are 1) the formation of thrombin via the prothrombinase complex, consisting of factor Va, Xa, and phospholipids, and 2) the subsequent proteolytic cleavage of fibrinogen by thrombin, which results in the generation of the insoluble fibrin clot matrix. Additionally, thrombin mediates platelet activation, thereby inducing their adhesion to the fibrin network. Inhibition or activation of enzymes in the coagulation cascade will thus influence blood-clotting events. Not surprisingly, thrombin, as a key player in the cascade, has been the subject of intensive pharmaceutical research, and numerous inhibitors of thrombin have been reported. An ideal thrombin inhibitor should be potent, orally bioavailable, and selective with regards to related serine proteases, such as trypsin.[7] However, finding an inhibitor that comprises both selectivity and suitable pharmacokinetics has been difficult to identify, prompting research to continue.[8–11]

The selectivity of small-molecule inhibitors toward a protein or enzyme target is often of crucial importance in the development of therapeutically useful molecules. Engineering high selectivity can be especially challenging when the site of interaction between the inhibitor and enzyme is

[a] E. L. Wu, Prof. K. L. Han
State Key Laboratory of Molecular Reaction Dynamics
Dalian Institute of Chemical Physics
Chinese Academy of Sciences, 457 Zhongshan Road
Dalian 116023 (China)
Fax: (+86) 411-8467-5584
E-mail: klhan@dicp.ac.cn

[b] Prof. J. Z. H. Zhang
Institute of Theoretical and Computational Chemistry
School of Chemistry and Chemical Engineering
Nanjing University, Nanjing 210093 (China)
Fax: (+86) 25-8368-6553
E-mail: zhang@itcc.nju.edu.cn
john.zhang@nyu.edu

[c] Prof. J. Z. H. Zhang
Department of Chemistry, New York University
New York, NY 10003 (USA)
Fax: (+1) 212-260-7905

within a highly homologous region of a large family of enzymes, such as the catalytic site of trypsin-like serine proteases.[12] As a member of the trypsin-like serine protease family, thrombin processes a catalytic site with high sequence homology and similar substrate specificity, therefore, their inhibitors need to be highly potent and selective among the closely related enzymes with adequate pharmacodynamic properties.[13] Selectivity relative to other serine protease inhibitors, particularly those that share thrombin's preference for P1 groups containing strong bases, such as guanidines and amidines, is a critical hurdle to overcome in the design of such a compound.[14] Trypsin (chosen as the benchmark serine protease) is arguably the most demanding serine protease in this regard owing to the similarity of their active sites and its location in the gut.[15]

Crystallographic investigations have revealed that thrombin is composed of disulfide-linked A and B chains.[16] It also has an anion-binding exosite positioned approximately 20 Å from the active site along a groove. The active site of thrombin is mainly defined by the specificity (S1) pocket, the hydrophobic proximal (S2) pocket, and the hydrophobic distal (S3) pocket. A schematic representation of the active site is shown in Figure 1.[8] The specificity pocket consists of

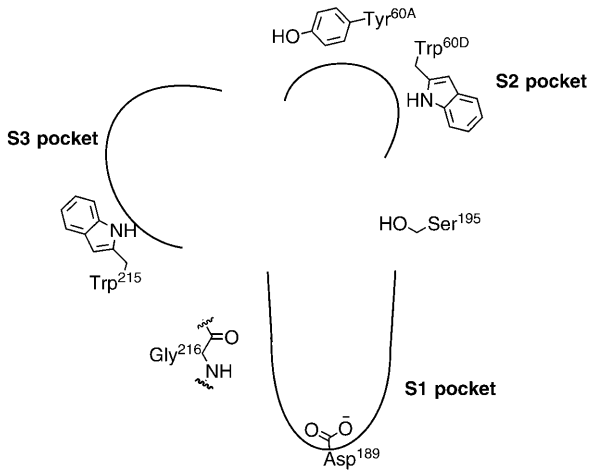

Figure 1. The schematic representation of the active site of thrombin.

a hydrophobic "channel" with the carboxylic acid of Asp189[17] and two backbone carbonyl groups in the bottom of the pocket. The former forms strong ionic interactions with amine-, guanidine-, or amidine-type structures located at the terminus of a hydrophobic spacer. The proximal pocket is defined on three sides by the Tyr60A and Trp60D side chains of the 60-insertion loop, the imidazole ring of His57, and the isobutyl group of Leu99 in the enzyme. The larger distal pocket is mainly made up of the side chains of Trp215, Ile174, and Leu99. Other important interactions with potential inhibitors include hydrogen bonding to the β-sheet segment from Ser214-Trp215-Gly216.[1] The catalytic triad of Asp102, His57, and Ser195 is responsible for the proteolytic activity.

Crystal structures of thrombin and trypsin have a considerable number of similarities but also some differences, which mediate the selectivity and are crucial in the design of selective thrombin inhibitors.[18] A focus in the design of selective thrombin inhibitors has been on the S1 pocket. Thrombin's S1 pocket is identical to that of trypsin except at residue 190, which is alanine or serine, respectively. Consequently the pocket is slightly larger and more lipophilic in thrombin than it is in trypsin.[19] The S2 pocket of thrombin is formed by an insertion loop and is lacking in trypsin, which is another structural difference. This proximal pocket is unique to thrombin and its occupancy by a stereoelectronically complementary group provides a significant contribution to the narrow substrate specificity of the enzyme.[10] These differences in the active site constitute a unique signature of each protease that can markedly affect the inhibitor-binding interactions and affinity even when the local sequences that form these sites are the same.[20,21]

The majority of available potent inhibitors generally show very poor oral bioavailability, bind strongly to plasma proteins, and/or do not have an appropriate plasma half-life after oral dosing.[22–24] Many of these pharmacokinetic problems are due to the high basicity of the first-generation thrombin inhibitors, which contain arginine or amidine-based S1 anchoring moieties. The high basicity of guanidine ($pK_a = 13$)/benzamidine ($pK_a = 11.6$) groups has translated into a high desolvation cost during passive absorption through the epithelial layer of the gut wall, which results in poor oral absorption. Overall, the short duration of action and poor oral absorption has precluded the development of these compounds as oral agents. As such, many pharmaceutical companies have invested significant efforts to identify less basic and neutral mimics to try to improve the pharmacokinetic properties of these compounds.[25]

In this study, molecular dynamics (MD) simulations followed by molecular mechanics generalized Born surface area (MM-GBSA)[26] analyses have been carried out to study the selectivity of two neutral and weakly basic P1 group inhibitors (177[27] and CDA[28]) with thrombin and trypsin. Both inhibitors exhibit excellent selectivity of thrombin versus trypsin despite the lack of a strong interaction with the specificity pocket.[27,28] Detailed binding free energies between these inhibitors and individual protein residues are calculated by using a per-residue basis decomposition method.[26] The analysis of detailed interaction energies provides insight on the protein–inhibitor-binding mechanism and helps elucidate the basis for achieving selectivity through interpretation of the structural and energetic results from the simulation. Thus, the study would be advantageous to produce small-molecule scaffolds of neutral and weakly basic P1 groups with greater intrinsic specificity toward thrombin and against anti-targets such as trypsin.

Computational Details

Thrombin system setups: Atomic coordinates of thrombin complexes were obtained from the Protein Data Bank (PDB). Two different crystal structures of thrombin bound to different inhibitors were used as starting structures in this study. The inhibitors are 177 (1AT6) and CDA (1MU6), which were designed and synthesized by Merck Research Laboratories (West Point, PA).[27,28] The structures of the two inhibitors are shown in Scheme 1. Protons were added to the system by using the Leap module of AMBER9.[29] In accordance with crystallographic conditions of the complexes, all ionizable side chains were configured in their characteristic ionized states at pH 7.3. The guanidine side chain of arginine and the terminal amino group of lysine were protonated, whereas the carboxy groups of aspartic and glutamic acid were deprotonated. The crystallographic water molecules in the PDB files were discarded and counterions were added to maintain the electroneutrality of the system. These starting structures were then placed in a truncated octahedral periodic box of TIP3P water molecules. The distance between the edges of the water box and the closest atom of solutes was at least 8 Å. The missing residues are simply ignored because they are all located far from the active site in the crystallographic structures.

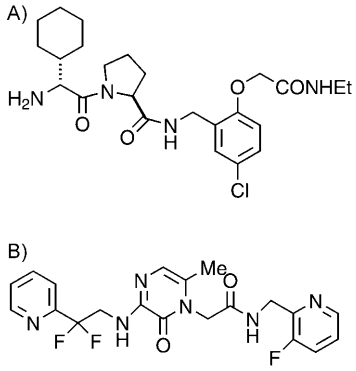

Scheme 1. Molecular structures of two inhibitors 177 (A) and CDA (B).

Atomic partial charges of the inhibitors were derived for this study by using the RESP method with the Antechamber module of AMBER9.[30] To obtain minimized geometries for electrostatic potential calculations, inhibitor geometries were first optimized with Gaussian 03 by using the Hartree-Fock/6-31G* level of theory.[31] Single-point calculations with Gaussion 03 were then performed to obtain the electrostatic potential around each compound by using the same basis set and level of theory as in the optimization step. Fitting charges to the electrostatic potential was performed with RESP.

The inhibitor of 177 was given a formal charge of +1 with a protonated amino group within the P3 group, whereas CDA was treated as neutral because the pyridine ring nitrogen atoms were relatively nonbasic owing to the strong electron-withdrawing effect of fluorin.[32]

Docking to trypsin: No crystallographic structure of trypsin complexed with 177 or CDA is currently available. Docking of 177/CDA to the active site of trypsin was performed with Autodock3[33] by using the genetic search algorithm. The initial structure of trypsin was taken from the crystal structure 1BTY,[34] and minimized to eliminate bad contacts. The two inhibitors were first placed in the binding site of the original inhibitor benzamidine, and $60\times60\times60$ grids with a step size of 0.375 Å were added with inhibitors at the center. After 200 docking runs, we choose structures based on the dock energy and cluster popularity for further molecular simulation studies, and system setup protocols are the same as the thrombin system. In Figure 2, we show the orientations of the two inhibitors in the thrombin and trypsin active sites with the MD lowest-energy structures.

MD simulations: The MD simulations were performed by using the AMBER9[29] suite of programs with the Parm99[35] force field to parametrize the protein. The system was minimized by steepest descent followed by conjugate gradient minimization. The particle mesh Ewald method[36] was used to treat long-range electrostatic interactions in a periodic boundary condition, and bond lengths involving bonds to hydrogen atoms were constrained by using SHAKE.[37] The time step for all MD simulations was 2 fs, with a direct-space, nonbonded cutoff of 10 Å. Applying position restraints with a force constant to all solute atoms and using the Langevin dynamics to control the temperature with a collision frequency of 1.0 ps^{-1}, 20 ps MD was carried out at constant volume, during which the system was heated from 0 to 300 K. A subsequent isothermal isobaric MD simulation was used for 5 ns to adjust the solvent density without any restraints on all the solute atoms. Finally, conformations were collected every 1 ps for the last 100 ps of the simulation, and 100 snapshots were collected for the MM-GBSA calculations.[26]

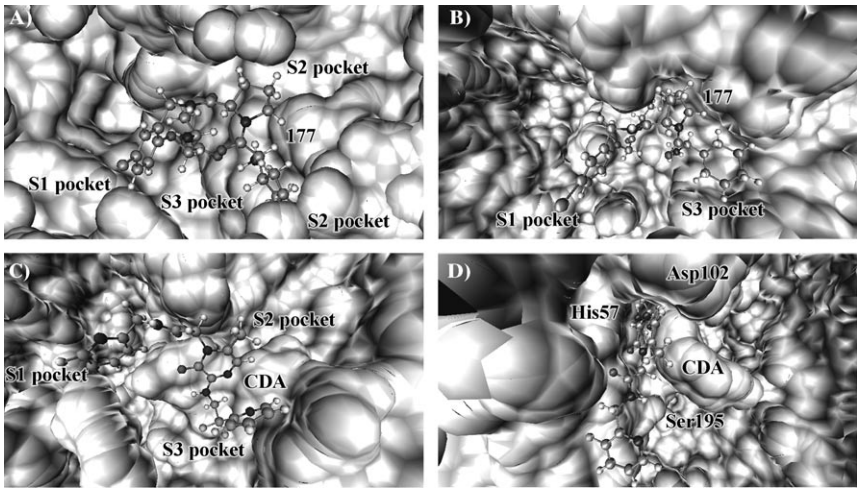

Figure 2. The orientations of 177 in the active site of A) thrombin and B) trypsin; and those of CDA in the active site of C) thrombin and D) trypsin.

Owing to the flexible nature of the inhibitors, it is incorrect to assume that the inhibitor conformations are the same in the bound state versus free in solution. The solution conformations of the inhibitors were determined with separate simulations.[38,39] Initial inhibitor conformations were taken directly from the corresponding complex structure. The inhibitors were then minimized and equilibrated by using the same protocols as described above. After 5 ns of MD simulations, the conformations generated from this set of simulations were also used for MM-GBSA calculations for comparison. Because thrombin and trypsin are relatively rigid proteins,[40] separate simulations for unbound proteins have not been performed owing to the large computational demand.

The MM-GBSA method: Although free energy perturbation (FEP) and thermodynamic integration (TI) calculations should give more accurate binding free energies, they are extremely time-consuming and require

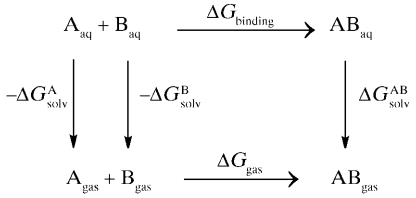

Figure 3. Thermodynamic cycle for the calculation of the absolute binding free energy. ΔG^{A}_{solv}, ΔG^{B}_{solv}, and ΔG^{AB}_{solv} are solvation free energy of A, B, and AB respectively. ΔG_{gas} and $\Delta G_{binding}$ are binding free energy in the gas phase and condensed phase, respectively.

sufficient statistical samplings. The heavy computational cost prevents FEP and TI from being routinely used for free energy calculations in structure-based drug design.[41–43] In this work, the binding free energy is calculated by using MM-GBSA[26] and normal-mode analysis. We chose 100 snapshots evenly from the last 100 ps MD simulation and calculate the binding free energies between the two inhibitors and thrombin/trypsin with MM-GBSA module in Amber9.[29] In MM-GBSA, the free energy of A+B→AB is calculated through the thermodynamic cycle,[43] as shown in Figure 3. The absolute binding free energy in the condensed phase can be calculated according to Equation (1):

$$\begin{aligned}\Delta G_{binding} &= \Delta G_{gas} - \Delta G^{A}_{solv} - \Delta G^{B}_{solv} + \Delta G^{AB}_{solv} \\ &= \Delta H_{gas} - T\Delta S - \Delta G^{A}_{GBSA} - \Delta G^{B}_{GBSA} + \Delta G^{AB}_{solv} \\ &= \Delta H_{gas} - T\Delta S + \Delta\Delta G_{GB} + \Delta\Delta G_{SA}\end{aligned} \quad (1)$$

The definition of various energy terms for Equation (1), are clear from Figure 3. ΔH_{gas} in Equation (1) is the total molecular mechanical energy in the gas phase, and it was calculated for the unsolvated molecule by using the standard Amber force field with the Sander module of the Amber9 program. The polar contribution to the free energy ($\Delta\Delta G_{GB}$) was calculated with the GB model developed by Onufriev and Case as implemented in AMBER9.[44] The nonpolar contribution to the solvation free energy ($\Delta\Delta G_{SA}$) owing to cavity formation and van der Waals interactions between the solute and solvent is estimated by a solvent-accessible surface area (SA) dependent term given in Equation (2):

$$\Delta G_{nonpolar} = \gamma SA \quad (2)$$

The SA was determined with the LCPO method[45] as implemented in AMBER9, and γ was set to 0.0072 kcal mol^{-1} Å^{-2}.[26]

Finally, entropy contributions arising from changes in the degrees of freedom (translational, rotational, and vibrational) of the solute molecules are included by applying classical statistical thermodynamics.[26] Because the normal-mode calculation of entropy is extremely time consuming for large systems, only 20 snapshots (every fifth snapshot of the 100 snapshots) for each inhibitor were used to estimate the contribution of the entropies to lower the computational cost. Contributions to the vibrational entropy are obtained by normal-mode analysis. After minimization of each snapshot in the gas phase by using the conjugated gradient method with a distance-dependent dielectric of $4r$ (in which r is the distance between two atoms) until the root-mean-square of the elements of the gradient vector is less than 10^{-4} kcal mol^{-1} Å^{-1}, frequencies of the vibrational modes are computed at 300 K for these minimized structures by using a harmonic approximation of the energies. The Nmode module of the AMBER9 package was used to perform this part of the calculation.[46]

Decomposition of free energies on a per-residue basis: Free energy decomposition in terms of contributions from structural subunits of both binding partners provides insight into the origin of binding on an atomic level. We demonstrated the decomposition of $\Delta G_{gas+solv}$ on a per-residue basis into contributions from van der Waals energy, the sum of coulomb interactions and polar solvation free energy and nonpolar contribution to solvation free energy for residues with $|\Delta G_{gas+solv}| \geq 1.5$ kcal mol^{-1}, and the contributions per residue were further subdivided into those from backbone atoms and those from side-chain atoms.[26] By providing a list of important or detrimental residues for the binding, and indications regarding the origin of their favorable or unfavorable role, the decomposition approach not only helps in selecting residues that are worth investigating, but also suggests some possible mutation.[47]

Hydrogen-bond analysis: A full analysis of all possible hydrogen bonds formed between the protein and inhibitors was carried out with the Ptraj subroutine of AMBER9.[26] We consider a hydrogen bond defined by distances of the heavy atoms of donor and acceptor of no more than 3.2 Å, and angles of donor and acceptor diatomic groups of no less than 120°.The occupancy of a hydrogen bond was computed by dividing the number of snapshots showing the hydrogen bond by the total number of snapshots along the MD trajectory.[48]

Results and Discussion

Inhibitor 177 binding to thrombin versus trypsin: To gain insights into different contributions to the affinity of protein–inhibitor binding, absolute binding free energies were computed for the thrombin–177 and trypsin–177 complexes. Table 1 lists contributions to binding free energy (i.e., gas-phase energies, solvation free energies, and contributions owing to changes in the translational, rotational, and vibra-

Table 1. Binding free energy components for the protein–inhibitor complex.

Contrib.[b]	Thrombin–177		Trypsin–177		Thrombin–CDA		Trypsin–CDA	
	Mean[a]	σ[c]	Mean[a]	σ[c]	Mean[a]	σ[c]	Mean[a]	σ[c]
ΔH_{elec}	−44.5(−59.2)[d]	0.3(0.8)	34.4(26.9)[d]	0.7(0.8)	−18.2(−18.6)[d]	0.4(1.3)	−21.5(−20.5)[d]	0.4(0.5)
ΔH_{vdW}	−66.7(−66.1)	0.2(0.4)	−51.3(−50.9)	0.3(0.4)	−54.5(−56.6)	0.2(1.1)	−36.9(−37.5)	0.3(0.4)
ΔH_{int}	0.0(4.4)	0.6(0.9)	0.0(3.5)	0.0(0.8)	−0.1(2.0)	0.0(2.3)	−0.1(2.4)	0.0(0.8)
ΔH_{gas}	−111.2(−120.9)	0.7(1.3)	−17.0(−20.5)	0.7(1.2)	−72.7(−73.2)	0.4(2.5)	−58.5(−55.6)	0.4(0.9)
ΔG_{np}	−7.4(−7.4)	0.0(0.0)	−5.6(−5.5)	0.0(0.0)	−6.7(−6.9)	0.0(0.0)	−5.8(−5.8)	0.0(0.0)
ΔG_{GB}	61.1(75.1)	0.2(0.7)	−22.8(−14.2)	0.5(0.6)	35.6(37.5)	0.3(1.0)	36.6(35.4)	0.3(0.4)
ΔG_{solv}	53.7(67.7)	0.2(0.7)	−28.4(−19.7)	0.5(0.6)	28.9(30.6)	0.3(1.0)	30.8(29.6)	0.3(0.4)
$\Delta G_{gas+solv}$	−57.4(−53.2)	0.6(−0.9)	−45.4(−40.2)	0.3(0.9)	−43.8(−42.6)	0.2(2.2)	−27.7(−25.9)	0.3(0.8)
ΔTS_{total}	−18.0(−18.3)	0.2(2.5)	−20.3(−20.9)	1.7(1.7)	−29.7(−30.9)	3.0(3.0)	−21.0(−20.7)	1.6(1.5)
ΔG_{total}	−38.8(−32.6)	2.2(3.0)	−25.4(−19.4)	2.3(3.8)	−14.9(−12.4)	3.0(3.9)	−7.1(−5.6)	1.3(3.0)

All values are given in kcal mol^{-1}. The standard state is taken to be 1 M. [a] Average over 100 (10 in the case of entropy contributions) snapshots of contribution(complex)–contribution(inhibitor)–contribution(protein). [b] Contribution: H_{elec}: coulombic energy; H_{vdW}: van der Waals energy; H_{int}: internal energy; $H_{gas}=H_{ele}+H_{vdW}+H_{int}$; G_{np}, nonpolar solvation free energy; G_{GB}, polar solvation free energy; $G_{solv}=G_{np}+G_{GB}$; $G_{gas+solv}=H_{gas}+G_{solv}$; TS_{total}, total entropy contribution; $G_{total}=G_{gas+solv}-TS_{total}$. [c] Standard error of mean values. [d] Contribution and standard error of mean values calculated from separate MD of inhibitors are shown in the parentheses.

tional degrees of freedom of the solute molecules) averaged over the MD trajectory for each protein–inhibitor complex, as well as contributions calculated from separate MD of inhibitors in the parentheses. The ideal mimicry of a binding event in vitro would be to run three separate simulations and calculate the energetic components of each. This would include the effects of the conformational changes upon binding, for example, protein and inhibitor flexibility.[49] We only ran the separate simulation of the inhibitor to obtain more reliable binding free energy considering the huge computational cost and relatively rigid protein structures.[40] As can be seen from Table 1, the binding free energy is -38.8 kcal mol^{-1} of the single simulation for the thrombin–177 complex and it changes to -32.6 kcal mol^{-1} after the separate inhibitor simulation correction. The relaxation energy of 177 is about 6.2 kcal mol^{-1} in the thrombin–177 complex. Similarly we obtained about 6.0 kcal mol^{-1} relaxation energy for the trypsin–177 complex, which is almost the same as that of the thrombin–177 complex.

The comparison between the calculated binding free energies and the experimental values are shown in Table 2. The

Table 2. Binding free energies [kcal mol^{-1}] and selectivity analysis from MM-GBSA calculation and experiment measurement for four protein–inhibitor complexes.

Complexes	Thrombin–177	Trypsin–177	Thrombin–CDA	Trypsin–CDA
ΔG_{total}	−38.8	−25.4	−14.9	−7.1
ΔG_{total} (sep MD)	−32.6	−19.4	−12.4	−5.6
ΔG_{bind} (exptl)[a]	−12.5	−6.4	−11.5	−4.9
$\Delta\Delta G$[b]	13.4		7.8	
$\Delta\Delta G$ (sep MD)[c]	13.2		6.8	
$\Delta\Delta G$ (exptl)[d]	6.1		6.6	

[a] Experimental data given as K_i values for all the complexes.[27,28] For direct comparison to calculated affinities, conversion to ΔG was estimated by $\Delta G = -RT\ln K_i$. [b] The difference between thrombin ΔG_{Thr} and trypsin ΔG_{Try}. [c] The difference of ΔG between thrombin and trypsin calculated from separated (sep) MD of inhibitors. [d] The difference of ΔG between thrombin and trypsin from experimental values.

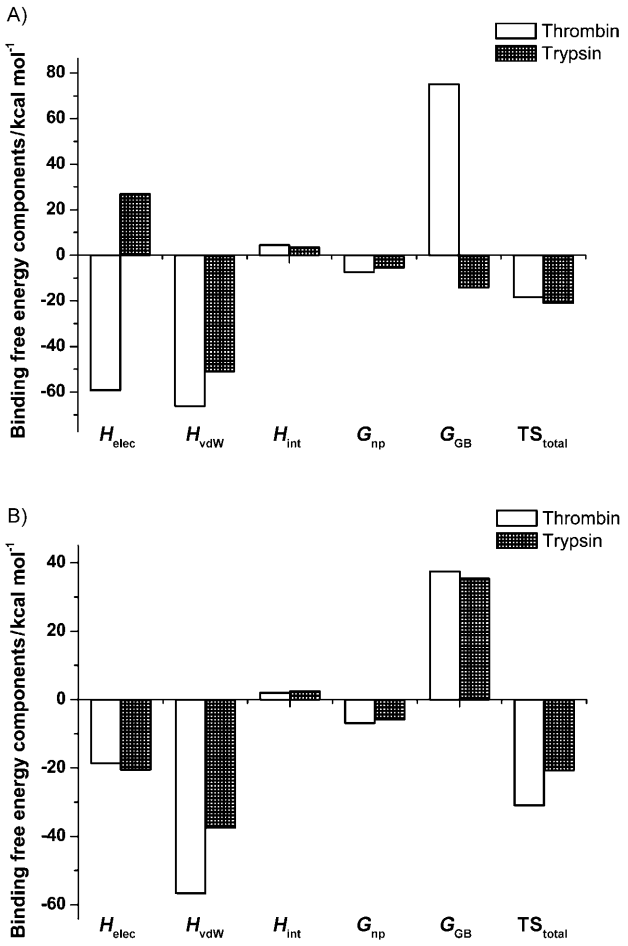

Figure 4. Comparison between the binding free energy components of A) thrombin–177 and trypsin–177 complexes, B) thrombin–CDA and trypsin–CDA complexes. H_{elec} = coloumbic energy, H_{vdW} = van der Waals energy, H_{int} = internal energy, G_{np} = nonpolar solvation free energy, G_{GB} = polar solvation free energy, and TS_{total} = total entropy contribution.

difference between $\Delta G_{thrombin}$ and $\Delta G_{trypsin}$ is used to analyze the selectivity for thrombin over trypsin. Our calculations correctly predict that 177 will bind more tightly to thrombin than trypsin. We also notice that the absolute values overestimate the binding affinities and the values of the calculated $\Delta\Delta G$ are about twice as much as the experimental data for 177. A likely explanation for this discrepancy is that large deviations in the coulombic and solvation terms are difficult to balance out effectively for charged inhibitors,[50] such as 177. Nevertheless, the calculated and experimental binding free energies of protein–177 complexes are highly correlated, and in fact, if the calculated binding energies are scaled by a factor of about 2.7, they will be in very good agreement with the experimental values.

To elucidate the mechanism driving the selective binding of 177 to thrombin over trypsin, we compared some independent binding free energy components between thrombin–177 and trypsin–177 complexes (Figure 4A). We found that the selectivity for thrombin over trypsin primarily originates from the contribution of van der Waals energy (ΔH_{vdW}), thus thrombin achieves better shape complementarity than trypsin with 177. The nonpolar solvation free energy (ΔG_{np}) also drives binding, which suggests better cavity packing. Although the internal energy (ΔH_{int}) and total entropy contribution (TS_{total}) are disfavorable for obtaining selectivity, the differences between thrombin–177 and trypsin–177 are very small, which indicates that they are less important factors for selectivity. The coulomb energy (ΔH_{elec}) and polar solvation free energy (G_{GB}) are highly anti-correlated and are approximately equal but opposite in sign for each complex because a large contribution to polar solvation free energy is the screening of the electrostatic interactions between the protein and the inhibitor.[51] The two competing effects nearly cancel each other and the selectivi-

ty of binding is thus dominated by the favorable van der Waals energy and nonpolar solvation free energy.[52]

To gain a more-detailed insight into the basis of the selectivity, structure and binding mode analyses have been performed to complement the energy analysis. The decomposition analysis generates a protein–inhibitor interaction spectrum showing binding interactions with individual residues as shown in Figure 5. The spectrum shows that the overwhelming majority of thrombin residues have negligible interaction with 177 (Figure 5A), and the dominant binding residues are Trp215, Gly216, Ser214, Cys191, Glu217, and Cys220 in order of reducing strength. Figure 6 and Table 3 show the decomposition of $\Delta G_{gas+solv}$ values on a per-residue basis into contributions from van der Waals energy, the sum of coulomb interactions, polar solvation free energy, and nonpolar contribution to solvation free energy for residues with $|\Delta G_{gas+solv}| \geq 1.5$ kcal mol^{-1} for four protein–inhibitor complexes. The contributions per residue were further subdivided into those from backbone atoms and those from side-chain atoms.[26] The sum of electrostatic interactions in the gas-phase plus the change of the polar part of the solvation free energy is shown instead of the separated contributions for the reason mentioned above. Figure 7 shows the relative position of the inhibitor in the binding complex with the residues to which it has strong interactions by using the lowest-energy structure extract from the MD trajectory. Hydrogen bonds observed are listed in Table 4 together with their occupancy during the 5 ns simulation. If more than one hydrogen bond is formed between two groups, only the largest occupancy value is reported.

The main binding attractions come from approximately six residues with individual $|\Delta G_{gas+solv}| \geq 1.5$ kcal mol^{-1} for the 177–thrombin complex (Figure 5A and Table 3). For all six residues, the van der Waals energy and nonpolar solvation energy are favorable for binding (Figure 6A). The dominating driving force of 177 binding to Trp215 is van der Waals energy, and the total van der Waals energy is -4.89 kcal mol^{-1} (Table 3). This result is in agreement with the strong hydrophobic and aromatic stacking interaction found between the P3 cyclohexyl ring moiety of 177 and the indole ring of Trp215 (Figure 7A). The N3 atom of 177 forms one hydrogen bond with the backbone carbonyl oxygen of Ser214, and the O1 and N1 atoms form two hydrogen bonds with Gly216 (Table 4 and Figure 7A). The distances between the corresponding oxygen and nitrogen atoms are 2.87, 2.88, and 2.85 Å, and thus the overall contribution of electrostatic energy is another important driving force for 177 binding to Ser214 and Gly216 (Figure 6A and Table 3). Additionally, the P1 aromatic ring contacts the sulfur atoms of Cys191–Cys220 disulfide linkage, forming a donor–π interaction similar to that observed in other groups[53] (Figure 7A), thus the van der Waals energy favors binding for these two residues. Although there is a strong ion-pair interaction between Glu217 and 177 (-17.89 kcal mol^{-1} in Table 3), the overall electrostatic energy disfavors the binding because of the penalty of the desolvation free energy (18.03 kcal mol^{-1} in Table 3).

The computed interaction spectrum in Figure 5B shows that the dominant interactions between 177 and trypsin are the bindings to Trp215, Gly216, Ser214, Leu99, and Gln192.

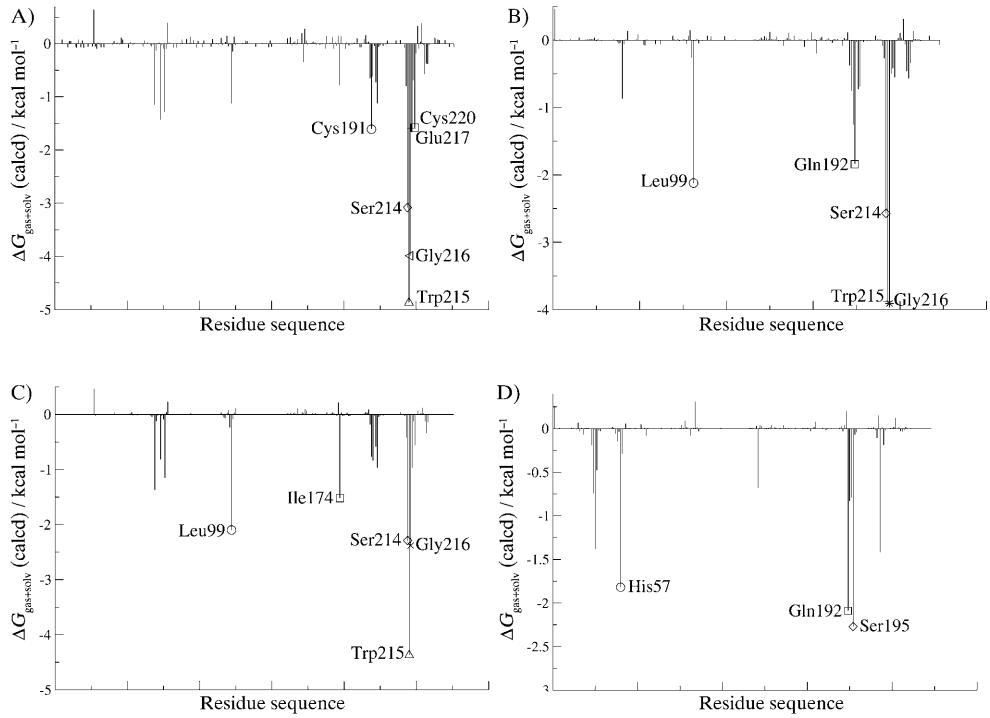

Figure 5. Decomposition of $\Delta G_{gas+solv}$ on a per-residue basis for the protein–inhibitor complex. A) thrombin–177; B) trypsin–177; C) thrombin–CDA; and D) trypsin–CDA.

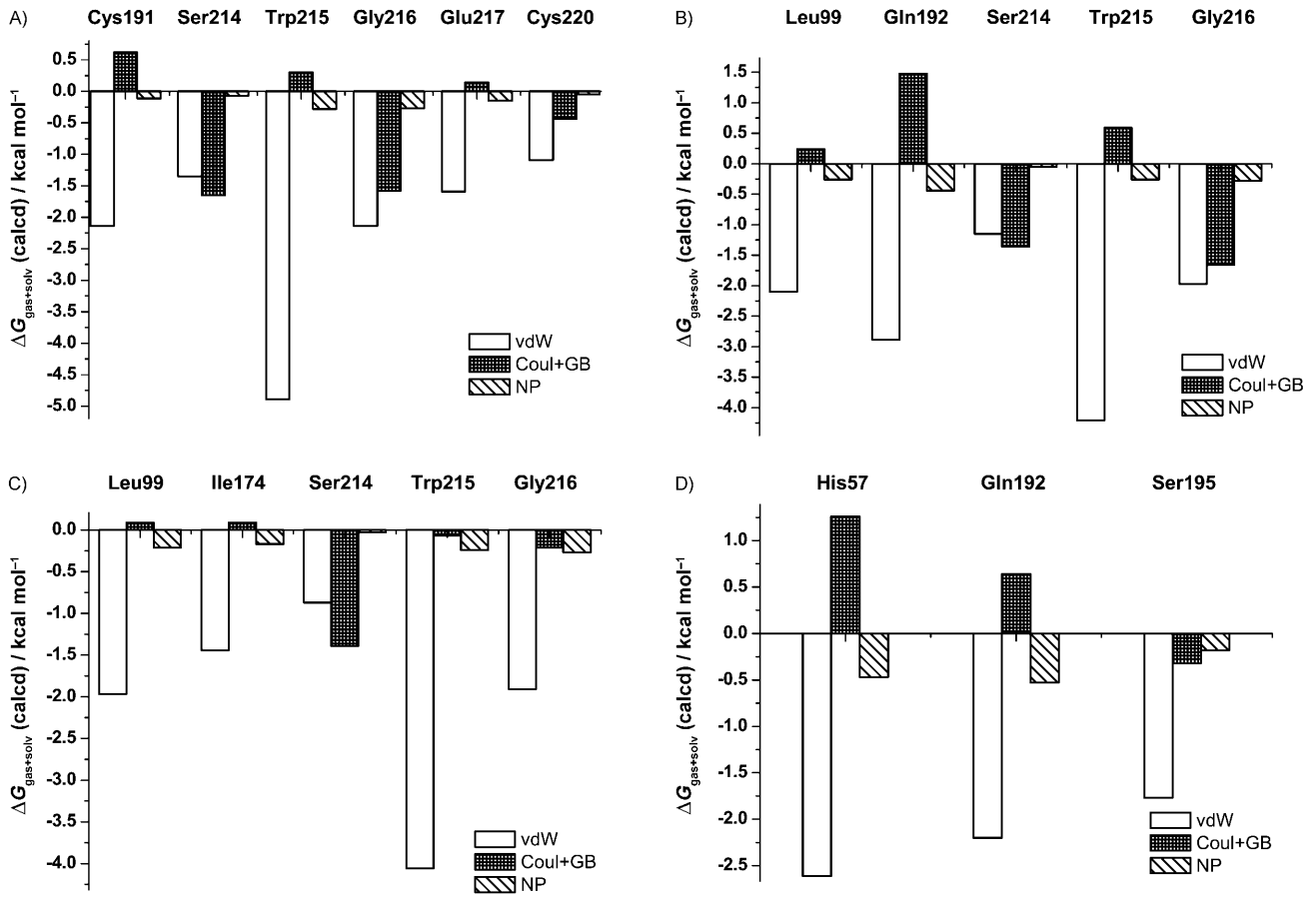

Figure 6. Decomposition of $\Delta G_{gas+solv}$ on a per-residue basis into contributions from the van der Waals energy (vdW), sum of Coulomb interactions and polar solvation free energy (Coul + GB), and the nonpolar (NP) part of solvation free energy for residues of protein–inhibitor complex for which $|\Delta G_{gas+solv}| \geq 1.5$ kcal mol^{-1}. A) thrombin–177; = B) trypsin–177; C) thrombin–CDA; and D) trypsin–CDA.

Table 3. Decomposition of $\Delta G_{gas+solv}$ (GBTOT) on a per-residue basis.[a]

Residue	S_{vdW}	B_{vdW}	T_{vdW}	S_{elec}	B_{elec}	T_{elec}	S_{GB}	B_{GB}	T_{GB}	T_{GBSUR}	T_{GBTOT}
thrombin–177											
Cys191	−0.62	−1.52	−2.14	−0.65	0.46	−0.19	0.42	0.40	0.81	−0.11	−1.61
Ser214	−0.17	−1.18	−1.35	0.52	−6.05	−5.53	−0.57	4.44	3.88	−0.07	−3.08
Trp215	−2.32	−2.57	−4.89	0.09	−0.64	−0.55	0.11	0.74	0.85	−0.28	−4.87
Gly216	0.00	−2.14	−2.14	0.00	−6.17	−6.17	0.00	4.59	4.59	−0.27	−3.99
Glu217	−0.54	−1.05	−1.59	−15.35	−2.53	−17.89	15.56	2.47	18.03	−0.15	−1.59
Cys220	−0.72	−0.38	−1.09	−0.92	0.05	−0.87	0.56	−0.13	0.43	−0.05	−1.58
trypsin–177											
Leu99	−1.82	−0.28	−2.10	1.91	−1.70	0.20	−1.63	1.68	0.04	−0.26	−2.12
Gln192	−1.79	−1.10	−2.89	−0.13	0.48	0.35	1.16	−0.02	1.13	−0.44	−1.84
Ser214	−0.15	−1.00	−1.15	−0.04	−5.42	−5.47	0.01	4.10	4.11	−0.05	−2.57
Trp215	−1.77	−2.43	−4.21	0.13	−0.33	−0.20	0.11	0.68	0.79	−0.26	−3.88
Gly216	0.00	−1.97	−1.97	0.00	−6.66	−6.66	0.00	5.00	5.00	−0.28	−3.91
thrombin–CDA											
Leu99	−1.68	−0.30	−1.97	0.27	−0.35	−0.07	−0.11	0.26	0.16	−0.21	−2.10
Ile174	−1.35	−0.09	−1.44	−0.01	0.06	0.04	0.04	0.01	0.05	−0.17	−1.52
Ser214	−0.13	−0.74	−0.87	−0.06	−2.50	−2.56	0.01	1.16	1.17	−0.03	−2.29
Trp215	−2.06	−1.99	−4.06	−0.36	−2.03	−2.39	0.25	2.07	2.32	−0.24	−4.37
Gly216	0.00	−1.91	−1.91	0.00	−2.11	−2.11	0.00	1.90	1.90	−0.27	−2.38
trypsin–CDA											
His57	−2.31	−0.30	−2.61	−1.14	0.46	−0.67	2.22	−0.28	1.93	−0.47	−1.82
Gln192	−1.27	−0.92	−2.20	−3.13	−2.11	−5.24	3.42	2.46	5.88	−0.53	−2.09
Ser195	−0.84	−0.94	−1.77	−1.05	0.10	−0.95	0.36	0.27	0.63	−0.18	−2.27

[a] Energies shown as contributions from van der Waals energy (vdW), coulomb interactions (elec), polar solvation free energy (GB), the nonpolar (GBSUR) part of solvation free energy of side chain atoms (S), backbone atoms (B), and sum of them (T) of protein–inhibitor complex. Only residues making a significant favorable or unfavorable contribution are shown ($|\Delta G_{gas+solv}| \geq 1.5$ kcal mol^{-1}). Energies are in kcal mol^{-1}.

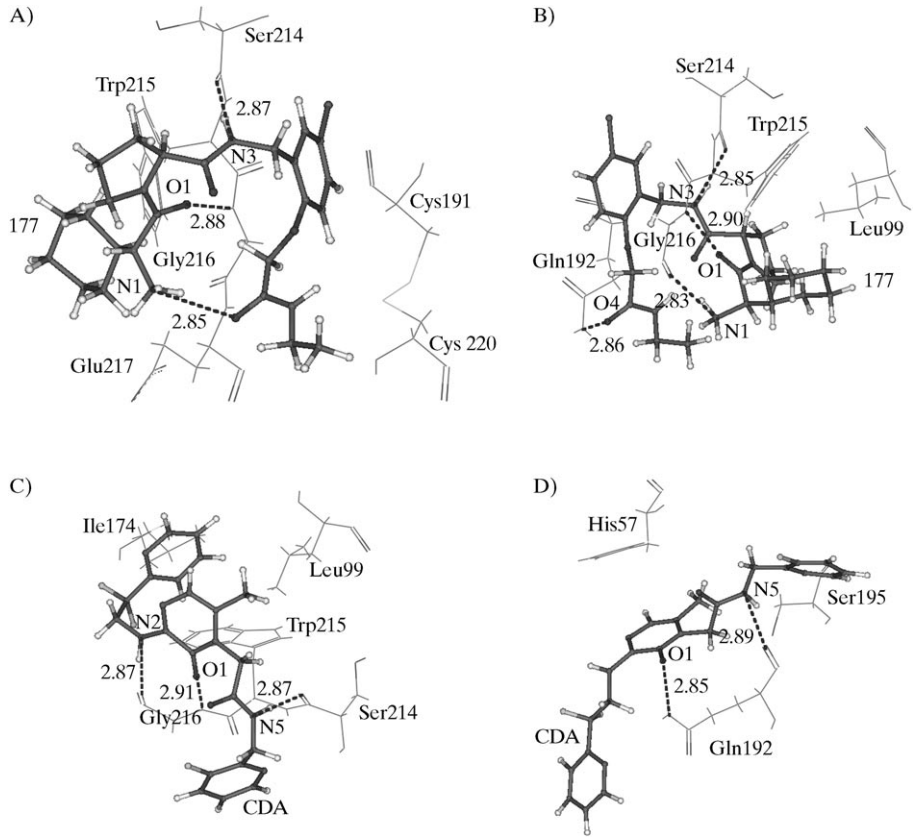

Figure 7. Some major interactions between the protein residues and the inhibitors with complex structures determined from the lowest-energy structures obtained from the MD simulation. The dashed line represents a hydrogen bond between the inhibitor and protein and its length. The inhibitor is shown in ball-and-stick representation. A) thrombin–177; B) trypsin/177; C) thrombin–CDA; D) trypsin–CDA.

Table 4. Hydrogen-bond formation between inhibitors and proteins.

Thrombin–177			Trypsin–177		
thrombin	177	occupancy[a]	trypsin	177	occupancy[a]
Ser214	N3[b]	65.43	Gln192	O4[b]	12.77
Gly216	O1	49.02	Ser214	N3	79.23
Gly216	N1	31.47	Gly216	O1	45.21
			Gly216	N1	24.13
thrombin–CDA			trypsin–CDA		
thrombin	CDA	occupancy	trypsin	CDA	occupancy
Ser214	N5[c]	66.47	Gln192	N5[c]	41.78
Gly216	N2	48.44	Gln192	O1	12.18
Gly216	O1	30.11			

Hydrogen bonds were defined by acceptor···donor atom distances of less than 3.2 Å and acceptor···H-donor angles of greater than 120°. Hydrogen bonds are reported only if they exit for greater than 10% of the investigated time period. [a] Occupancy is in units of percentage of the investigated time period. If more than one hydrogen bond is formed between the donor and acceptor, only the largest occupancy value is reported. [b] Atom name of 177. [c] Atom name of CDA

By comparing results in Figure 6B and geometries in Figure 7B, we can explain the binding character of 177 to trypsin as follows: As in thrombin–177 binding, the van der Waals and nonpolar solvation energies are all favorable for 177 binding to these five residues, and the contribution of nonpolar solvation energy is much smaller than that of van der Waals energy. Similar to thrombin, inhibitor 177 also forms one hydrogen bond to the backbone carbonyl oxygen of Ser214, two hydrogen bonds to Gly216 of trypsin in an antiparallel β-strand fashion, and the distances between the donor and acceptor are shown in Figure 7B. Both the van der Waals and overall electrostatic energies favor binding for these two residues. There is also significant aromatic stacking interaction ($-4.21\,kcal\,mol^{-1}$ in Table 3) between 177 and Trp215, and the van der Waals energy is $-2.10\,kcal\,mol^{-1}$ between 177 and Leu99. Besides the van der Waals energy of $-2.89\,kcal\,mol^{-1}$, an unstable hydrogen bond is formed between the O4 atom of 177 and Gln192 with an occupancy percentage of 12.77 (Table 4) from the simulation. The overall electrostatic energy of Gln192 disfavors binding to 177, because the favorable electrostatic interaction in the gas-phase is offset by the desolvation free energy required.

Based on the energy and structure analysis above, we believe that the selectivity of 177 arises from the difference in van der Waals and nonpolar solvation energies, and the van der Waals energy is the dominant factor. We also notice that 177 binds to thrombin and trypsin in a similar binding mode, and it primarily binds to the antiparallel β-strand segment of Ser214-Trp215-Gly216 and adjacent residues.

Inhibitor CDA binding to thrombin versus trypsin: Compared with the protein–177 complex, the computational results of the absolute binding free energy for the protein–CDA complex agree well with the experimental values (Tables 1 and 2) in an absolute scale ($-14.9\,kcal\,mol^{-1}$ for thrombin and $-7.1\,kcal\,mol^{-1}$ for trypsin). The reason for this is that CDA is treated as neutrally charged, whereas 177 is protonated, and reliable solvation energy of a charged inhibitor is not easy to calculate at present. The calculated $\Delta\Delta G$ between thrombin and trypsin ($7.8\,kcal\,mol^{-1}$ in Table 2) was also found to be in accordance with the experimental data ($6.6\,kcal\,mol^{-1}$ in Table 2). Considering that the separate inhibitor simulation correction, both the absolute values ($-12.4\,kcal\,mol^{-1}$ for thrombin and $-5.6\,kcal\,mol^{-1}$ for trypsin) and the calculated $\Delta\Delta G$ ($6.8\,kcal\,mol^{-1}$ in

Table 2) are improved, although the relaxation energies are not as large as those of the 177 complexes.

Comparison between the free energy components of thrombin–CDA and trypsin–CDA complexes was performed to understand the mechanism driving binding selectivity. Figure 4B shows that selectivity originates from the van der Waals energy, the total entropy contribution, and nonpolar solvation energy. Similar to the 177 complexes, the van der Waals energy is also the dominant factor responsible for different binding affinity between thrombin and trypsin. The overall contribution of the electrostatic energy is not in favor of the selectivity.

Decomposition analysis suggests that five residues play key roles for CDA binding to thrombin, and they are Trp215, Gly216, Ser214, Leu99, and Ile174 (Table 3 and Figure 5C). For all of the residues, van der Waals and nonpolar solvation energies are favorable for binding, except for the vanishing nonpolar solvation energy of Ser214 (Figure 6C). The antiparallel β-strand hydrogen bonding motif between the aminopyrazinone and Gly216 is maintained; similarly the Ser214 hydrogen bond to the inhibitor amide is conserved.[28] The distances between the donor and acceptor are 2.87, 2.91, and 2.87 Å, as shown in Table 4 and Figure 7C. Besides the van der Waals energy, the overall electrostatic energy of Ser214 also makes a significant contribution to binding, even larger than the contribution of van der Waals interactions. For the other three residues in the S3 pocket (Trp215, Leu99, and Ile174), van der Waals energy is found to be the main energy term favoring binding. With the most favorable van der Waals energy of $-4.06\ \mathrm{kcal\,mol^{-1}}$ (Table 3), CDA makes the edge-to-face σ–π interaction between the P3 aryl group and the π-rich Trp215 further reinforced by the incorporation of the electron-deficient P3 pyridine.[28]

The residues responsible for CDA binding to trypsin are Ser195, Gln192, and His57 as shown in the interaction spectrum shown in Figure 5D. For Ser195, favorable contribution to binding affinity mostly arises from van der Waals energy ($-1.77\ \mathrm{kcal\,mol^{-1}}$ in Table 3 and Figure 6D).The overall electrostatic energy and nonpolar solvation energy provide the additional increase in binding energy, but much smaller. CDA makes two hydrogen bonds with Gln192 (Table 4 and Figure 7D), but the favorable coulomb interactions are also compensated by unfavorable contributions from polar solvation free energy, thus van der Waals energy provides the driving force for binding. Further stabilization is provided by the van der Waals energy of $-2.61\ \mathrm{kcal\,mol^{-1}}$ (Table 3) owing to the favorable interaction between the imidazole ring of His57 and aminopyrazinone moiety of CDA, although the overall contribution of electrostatic energy of His57 is disfavorable for binding.

To summarize, the present results show that the selectivity of CDA binding to thrombin over trypsin originates from the van der Waals energy, nonpolar solvation energy, and the total entropy contribution. As is the case for 177, the van der Waals energy is the dominant factor for selectivity. Notably, CDA binds to thrombin and trypsin in very different modes. Specifically, CDA binds to the antiparallel β strand (Ser214 and Gly216) and S3 pocket residues (Trp215, Leu99, and Ile174) of thrombin, whereas it binds to the catalytic triad of trypsin (Ser195 and His57) and the residues in the vicinity of them.

Conclusion

We used MD simulations in conjunction with free-energy analysis by using the MM-GBSA method to analyze the basis of selectivity of two inhibitors, and also provide insight into the protein–inhibitor-binding mechanism. In particular, inhibitors were selected to exclude the strong basic P1 motif, such as an amidine or guanidine, and instead to focus on identifying hits with better druglike properties. We also performed a separate MD simulation of the inhibitor to include the effects of the conformational changes upon binding. The computed absolute values of binding free energies of protein–CDA complexes are in good accordance with experimental data, whereas those of the protein–177 complex overestimate binding. This is likely to be owing to the fact that the large deviations in the Coulombic and solvation terms are difficult to balance effectively for charged inhibitors.[50]

In each case, the simulation results correctly predict that a given inhibitor will bind more tightly to thrombin than trypsin. The decomposition analysis shows that the dominant factor of selectivity of the two inhibitors is van der Waals energy, which suggests better shape complementarity and packing. Most of the favorable coulomb interactions are offset by unfavorable contributions from polar solvation free energy, so the overall contribution of electrostatic energy provides no direct thermodynamic advantage for selectivity, or even oppose achieving it. Some other free energy components of nonpolar solvation free energy and total entropy contribution are also in favor of achieving selectivity, but the contributions are much smaller.

Binding mode and structure analyses indicate that 177 binds to thrombin and trypsin in a similar binding mode, and it primarily binds to the antiparallel β-strand segment of Ser214-Trp215-Gly216 and adjacent residues, whereas CDA binds to thrombin and trypsin in very different modes. CDA binds to the antiparallel β strand (Ser214, and Gly216) and S3 pocket residues (Trp215, Leu99 and Ile174) of thrombin, but it binds to the catalytic triad of trypsin (Ser195 and His57) and nearby residues. Based on the analysis above, the higher selectivity of CDA is likely to be owing to the different binding mode between thrombin and trypsin, which results in a greater difference in the binding free energy.

By accurately modeling known thrombin–inhibitor systems and analyzing the structure information, selective and potent thrombin inhibitors may be proposed with greater confidence. The information gained from this study should help lead to the discovery of new inhibitors with improved binding properties.

Acknowledgements

We thank the supercomputer center of Virtual Laboratory of Computational Chemistry, Computer Network Information Center, Chinese Academy of Sciences for the computational resources. This work is partially supported by the National Science Foundation of China (Grant no. 20773060), National Key Basic Research Special Fund (Grant no. 2007CB815202), and NYU Research Challenge Fund.

[1] J. W. Nilsson, I. Kvarnstrom, D. Musil, I. Nilsson, B. Samulesson, *J. Med. Chem.* **2003**, *46*, 3985–4001.
[2] J. E. Reiner, D. V. Siev, G. L. Araldi, J. R. J. Cui, J. Z. Ho, K. M. Reddy, L. Mamedova, P. H. Vu, K. S. S. Lee, N. K. Minami, T. S. Gibson, S. M. Anderson, A. E. Bradbury, T. G. Nolan, J. E. Semple, *Bioorg. Med. Chem. Lett.* **2002**, *12*, 1203–1208.
[3] S. J. Gardell, P. E. J. Sanderson, *Coron. Heart Dis.* **1998**, *9*, 75–81.
[4] P. E. J. Sanderson, K. J. Cutrona, D. L. Dyer, J. A. Krueger, L. C. Kuo, S. D. Lewis, B. J. Lucas, Y. W. Yan, *Bioorg. Med. Chem. Lett.* **2003**, *13*, 161–164.
[5] J. A. Shafer, *Curr. Opin. Chem. Biol.* **1998**, *2*, 458–465.
[6] G. P. Vlasuk, *Arch. Pathol. Lab. Med.* **1998**, *122*, 812–814.
[7] U. E. W. Lange, D. Baucke, W. Hornberger, H. Mack, W. Seitza, H. W. Hoffken, *Bioorg. Med. Chem. Lett.* **2003**, *13*, 2029–2033.
[8] A. Linusson, J. Gottfries, T. Olsson, E. Ornskov, S. Folestad, B. Norden, S. Wold, *J. Med. Chem.* **2001**, *44*, 3424–3439.
[9] K. Menear, *Curr. Med. Chem.* **1998**, *5*, 457–468.
[10] U. Obst, D. W. Banner, L. Weber, F. Diederich, *Chem. Biol.* **1997**, *4*, 287–295.
[11] P. E. J. Sanderson, *Med. Res. Rev.* **1999**, *19*, 179–197.
[12] R. L. Mackman, B. A. Katz, J. G. Breitenbucher, H. C. Hui, E. Verner, C. Luong, L. Liu, P. A. Sprengeler, *J. Med. Chem.* **2001**, *44*, 3856–3871.
[13] B. A. Bhongade, V. V. Gouripur, A. K. Gadad, *Bioorg. Med. Chem.* **2005**, *13*, 2773–2782.
[14] M. R. Wiley, M. J. Fisher, *Expert Opin. Ther. Pat.* **1997**, *7*, 1265–1282.
[15] P. E. J. Sanderson, M. G. Stanton, B. D. Dorsey, T. A. Lyle, C. McDonough, W. M. Sanders, K. L. Savage, A. M. Naylor-Olsen, J. A. Krueger, S. D. Lewis, B. J. Lucas, J. J. Lynch, Y. W. Yan, *Bioorg. Med. Chem. Lett.* **2003**, *13*, 795–798.
[16] D. K. JonesHertzog, W. L. Jorgensen, *J. Med. Chem.* **1997**, *40*, 1539–1549.
[17] W. Bode, I. Mayr, U. Baumann, R. Huber, S. R. Stone, J. Hofsteenge, *EMBO J.* **1989**, *8*, 3467–3475.
[18] G. Mlinsek, M. Novic, M. Kotnik, T. Solmajer, *J. Chem. Inf. Comput. Sci.* **2004**, *44*, 1872–1882.
[19] Z. G. Chen, Y. Li, A. M. Mulichak, S. D. Lewis, J. A. Shafer, *Arch. Biochem. Biophys.* **1995**, *322*, 198–203.
[20] B. A. Katz, K. Elrod, E. Verner, R. L. Mackman, C. Luong, W. D. Shrader, M. Sendzik, J. R. Spencer, P. A. Sprengeler, A. Kolesnikov, V. W. F. Tai, H. C. Hui, G. Breitenbucher, D. Allen, J. W. Janc, *J. Mol. Biol.* **2003**, *329*, 93–120.
[21] B. A. Katz, R. Mackman, C. Luong, K. Radika, A. Martelli, P. A. Sprengeler, J. Wang, H. D. Chan, L. Wong, *Chem. Biol.* **2000**, *7*, 299–312.
[22] G. De Simone, V. Menchise, S. Omaggio, C. Pedone, A. Scozzafava, C. T. Supuran, *Biochemistry* **2003**, *42*, 9013–9021.
[23] J. Hauptmann, J. Sturzebecher, *Thromb. Res.* **1999**, *93*, 203–241.
[24] D. Leung, G. Abbenante, D. P. Fairlie, *J. Med. Chem.* **2000**, *43*, 305–341.
[25] P. Y. S. Lam, C. G. Clark, R. H. Li, D. J. P. Pinto, M. J. Orwat, R. A. Galemmo, J. M. Fevig, C. A. Teleha, R. S. Alexander, A. M. Smallwood, K. A. Rossi, M. R. Wright, S. A. Bai, K. He, J. M. Luettgen, P. C. Wong, R. M. Knabb, R. R. Wexler, *J. Med. Chem.* **2003**, *46*, 4405–4418.
[26] H. Gohlke, C. Kiel, D. A. Case, *J. Mol. Biol.* **2003**, *330*, 891–913.
[27] T. J. Tucker, S. F. Brady, W. C. Lumma, S. D. Lewis, S. J. Gardell, A. M. Naylor-Olsen, Y. W. Yan, J. T. Sisko, K. J. Stauffer, B. J. Lucas, J. J. Lynch, J. J. Cook, M. T. Stranieri, M. A. Holahan, E. A. Lyle, E. P. Baskin, I. W. Chen, K. B. Dancheck, J. A. Krueger, C. M. Cooper, J. P. Vacca, *J. Med. Chem.* **1998**, *41*, 3210–3219.
[28] C. S. Burgey, K. A. Robinson, T. A. Lyle, P. E. J. Sanderson, S. D. Lewis, B. J. Lucas, J. A. Krueger, R. Singh, C. Miller-Stein, R. B. White, B. Wong, E. A. Lyle, P. D. Williams, C. A. Coburn, B. D. Dorsey, J. C. Barrow, M. T. Stranieri, M. A. Holahan, G. R. Sitko, J. J. Cook, D. R. McMasters, C. M. McDonough, W. M. Sanders, A. A. Wallace, F. C. Clayton, D. Bohn, Y. M. Leonard, T. J. Detwiler, J. J. Lynch, Y. W. Yan, Z. G. Chen, L. Kuo, S. J. Gardell, J. A. Shafer, J. P. Vacca, *J. Med. Chem.* **2003**, *46*, 461–473.
[29] D. A. Case, T. A. Darden, I. T. E. Cheatham, C. L. Simmerling, J. Wang, R. E. Duke, R. Luo, K. M. Merz, D. A. Pearlman, M. Crowley, R. C. Walker, W. Zhang, S. B. Wang, A. R. Hayik, G. Seabra, K. F. Wong, F. Paesani, X. Wu, S. Brozell, V. Tsui, H. Gohlke, L. Yang, C. Tan, J. Mongan, V. Hornak, G. Cui, P. Beroza, D. H. Mathews, C. Schafmeister, W. S. Ross, P. A. Kollman, AMBER 9, **2006**.
[30] C. I. Bayly, P. Cieplak, W. D. Cornell, P. A. Kollman, *J. Phys. Chem.* **1993**, *97*, 10269–10280.
[31] Gaussian 03, Revision C.02, M. J. Frisch, G. W. Trucks, H. B. Schlegel, G. E. Scuseria, M. A. Robb, J. R. Cheeseman, J. A. Montgomery, Jr., T. Vreven, K. N. Kudin, J. C. Burant, J. M. Millam, S. S. Iyengar, J. Tomasi, V. Barone, B. Mennucci, M. Cossi, G. Scalmani, N. Rega, G. A. Petersson, H. Nakatsuji, M. Hada, M. Ehara, K. Toyota, R. Fukuda, J. Hasegawa, M. Ishida, T. Nakajima, Y. Honda, O. Kitao, H. Nakai, M. Klene, X. Li, J. E. Knox, H. P. Hratchian, J. B. Cross, V. Bakken, C. Adamo, J. Jaramillo, R. Gomperts, R. E. Stratmann, O. Yazyev, A. J. Austin, R. Cammi, C. Pomelli, J. W. Ochterski, P. Y. Ayala, K. Morokuma, G. A. Voth, P. Salvador, J. J. Dannenberg, V. G. Zakrzewski, S. Dapprich, A. D. Daniels, M. C. Strain, O. Farkas, D. K. Malick, A. D. Rabuck, K. Raghavachari, J. B. Foresman, J. V. Ortiz, Q. Cui, A. G. Baboul, S. Clifford, J. Cioslowski, B. B. Stefanov, G. Liu, A. Liashenko, P. Piskorz, I. Komaromi, R. L. Martin, D. J. Fox, T. Keith, M. A. Al-Laham, C. Y. Peng, A. Nanayakkara, M. Challacombe, P. M. W. Gill, B. Johnson, W. Chen, M. W. Wong, C. Gonzalez, J. A. Pople, Gaussian, Inc., Wallingford CT, **2004**.
[32] C. S. Burgey, K. A. Robinson, T. A. Lyle, P. G. Nantermet, H. G. Selnick, R. C. A. Isaacs, S. D. Lewis, B. J. Lucas, J. A. Krueger, R. Singh, C. Miller-Stein, R. B. White, B. Wong, E. A. Lyle, M. T. Stranieri, J. J. Cook, D. R. McMasters, J. M. Pellicore, S. Pal, A. A. Wallace, F. C. Clayton, D. Bohn, D. C. Welsh, J. J. Lynch, Y. W. Yan, Z. G. Chen, L. Kuo, S. J. Gardell, J. A. Shafer, J. P. Vacca, *Bioorg. Med. Chem. Lett.* **2003**, *13*, 1353–1357.
[33] G. M. Morris, D. Goodsell, R. S.; Huey, W. E. Hart, S. Halliday, R. Belew, A. J. Olson, AutoDock 3.0, **1999**.
[34] B. A. Katz, J. Finermoore, R. Mortezaei, D. H. Rich, R. M. Stroud, *Biochemistry* **1995**, *34*, 8264–8280.
[35] J. M. Wang, P. Cieplak, P. A. Kollman, *J. Comput. Chem.* **2000**, *21*, 1049–1074.
[36] T. Darden, D. York, L. Pedersen, *J. Chem. Phys.* **1993**, *98*, 10089–10092.
[37] J. P. Ryckaert, G. Ciccotti, H. J. C. Berendsen, *J. Comput. Phys.* **1977**, *23*, 327–341.
[38] K. M. Masukawa, P. A. Kollman, I. D. Kuntz, *J. Med. Chem.* **2003**, *46*, 5628–5637.
[39] H. Gohlke, D. A. Case, *J. Comput. Chem.* **2004**, *25*, 238–250.
[40] H. Gohlke, G. Klebe, *Angew. Chem. Int. Ed.* **2002**, *41*, 2645–2676.
[41] D. L. Beveridge, F. M. Dicapua, *Annu. Rev. Biophys. Biophys. Chem.* **1989**, *18*, 431–492.
[42] P. Kollman, *Chem. Rev.* **1993**, *93*, 2395–2417.
[43] J. M. Wang, P. Morin, W. Wang, P. A. Kollman, *J. Am. Chem. Soc.* **2001**, *123*, 5221–5230.
[44] A. Onufriev, D. Bashford, D. A. Case, *Proteins Struct. Funct. Bioinf.* **2004**, *55*, 383–394.
[45] J. Weiser, P. S. Shenkin, W. C. Still, *J. Comput. Chem.* **1999**, *20*, 217–230.
[46] D. A. Pearlman, *J. Med. Chem.* **2005**, *48*, 7796–7807.

[47] V. Zoete, O. Michielin, *Proteins Struct. Funct. Bioinf.* **2007**, *67*, 1026–1047.
[48] S. Huo, I. Massova, P. A. Kollman, *J. Comput. Chem.* **2002**, *23*, 15–27.
[49] J. M. J. Swanson, R. H. Henchman, J. A. McCammon, *Biophys. J.* **2004**, *86*, 67–74.
[50] B. A. Tounge, R. T. Rajarnani, E. W. Baxter, A. B. Reitz, C. H. Reynolds, *J. Mol. Graphics Modell.* **2006**, *24*, 475–484.
[51] F. Grater, S. M. Schwarzl, A. Dejaegere, S. Fischer, J. C. Smith, *J. Phys. Chem. B* **2005**, *109*, 10474–10483.
[52] R. C. Rizzo, S. Toba, I. D. Kuntz, *J. Med. Chem.* **2004**, *47*, 3065–3074.
[53] M. B. Young, J. C. Barrow, K. L. Glass, G. F. Lundell, C. L. Newton, J. M. Pellicore, K. E. Rittle, H. G. Selnick, K. J. Stauffer, J. P. Vacca, P. D. Williams, D. Bohn, F. C. Clayton, J. J. Cook, J. A. Krueger, L. C. Kuo, S. D. Lewis, B. J. Lucas, D. R. McMasters, C. Miller-Stein, B. L. Pietrak, A. A. Wallace, R. B. White, B. Wong, Y. W. Yan, P. G. Nantermet, *J. Med. Chem.* **2004**, *47*, 2995–3008.

Received: February 14, 2008
Published online: August 4, 2008

